Mechanical Systems and Signal Processing 66-67 (2016) 339–348

Contents lists available at ScienceDirect

Mechanical Systems and Signal Processing

journal homepage: www.elsevier.com/locate/ymssp

Time–frequency processing of track irregularities in high-speed train

Jing Ning [a,*], Jianhui Lin [b], Bing Zhang [b]

[a] School of Mechanical Engineering, Southwest Jiaotong University, Chengdu 610031, Sichuan Province, China
[b] National Traction Power Laboratory, Southwest Jiaotong University, Chengdu 610031, Sichuan Province, China

ARTICLE INFO

Article history:
Received 9 June 2013
Received in revised form
15 April 2015
Accepted 24 April 2015
Available online 26 June 2015

Keywords:
Axle box acceleration
Time–frequency distribution
Detection
Rail irregularities

ABSTRACT

Track irregularities are the main source of vehicle vibration. With the increase in the speed, the track irregularities have become a more significant issue of concerned. The axle box acceleration signals can be obtained for analyzing the track irregularities, but the signals are usually non-stationary and signal processing results are not normally satisfied with the ordinary way. Thus, time–frequency distribution analysis is proposed to use in this study. To minimize the cross-terms, a new method based on Empirical Mode Decomposition (EMD) and Cohen's class distribution has been developed and advanced. This approach has been tested with three typical simulation signals and then applied to analyze the track irregularities. The result is consistent with the result from track inspection cars. This indicates this new algorithm is suitable for analyzing the track irregularities. It can be applied in rail irregularity measurement to compensate some shortages of the track inspection cars.

1. Introduction

With the increase of the train speed, the track quality becomes the main concerns for transportation safety. The track inspection cars are the main devices for the track maintenance. The inertial reference systems [1,2] and the CCD optical systems [3] are used in track inspection cars. But the costs of using special devices are very high. Besides, their maintenance also cost special service time because in-service trains must stop for the track monitor [4]. So a quick rail inspection strategy with axle box acceleration (ABA) signals were proposed in [5,6]. There are many advantages associated to this method. Firstly, ABA measurement does not need sophisticated instrumentation, and accelerometers can be easily fixed to the outside of the axle box [7]. Secondly, the track irregularities monitor processing can be executed in the normal working state in high-speed. It opens a door for monitoring the track quality daily.

Nowadays, monitoring the track irregularities by axle box acceleration is progressing gradually. In Spain and Italy, metropolitan railway systems are in great demand. Acceleration signals from the axle box, bogies, and vehicle bodies of Spanish high-speed trains (AVE) are used to analyze the deterioration process in track geometric quality [8]. And a developed system which could record vertical accelerations from the bogies of in-service railway vehicles is also in service [9]. In Italy, the public transportation company in Milan set up a cooperative project with Politecnico di Milano to develop the axle box accelerometer system for track condition inspection [4,10]. In Netherlands, the possible use of axle box

* Corresponding author. Tel.: +86 28 87634693; fax: +86 28 87600690.
E-mail address: ningjing@swjtu.edu.cn (J. Ning).

http://dx.doi.org/10.1016/j.ymssp.2015.04.031
0888-3270/

acceleration for condition monitoring of welds was proposed in [11,12], and a weld was simulated through finite-element modeling [7]. In Sweden, the field measurement of vertical wheel–rail contact forces in the frequency range of 0–2000 Hz was reported [13]. In Korea, a mixed filtering approach was proposed for stable displacement estimation [14]. In this approach, a state-space model and Kalman filter were used, and the system was supposed to be stable. In China, some measurement devices were also appeared in high-speed EMUs (Electric Multiple Units). And the signal processing methods have made progress in recent years. But all these methods assume that the signals are stable, which is inconsistent with the objective facts [15–19].

The axle box acceleration signals are non-stationary signals, containing complex vibration components. The signals are non-uniformly sampled. But retrieval results show that the methods used in this field are usually for stationary signals, and there is no commercial solution for monitoring track irregularities in high-speed train by ABA. So a suitable algorithm for the track irregularities monitoring in non-stationary high-speed state has remained elusive. Time–frequency representations (TFRs) are an ideal method for non-stationary signals. But cross-terms have been the main obstacle preventing the use of the TFRs. Using a method named Empirical Mode Decomposition (EMD) [18], signals can be decomposed of the source data into a finite set of Intrinsic Mode Functions (IMFs). This is a new method to analyze the signals for non-stationary time series. In order to minimize the cross-term interference in TFRs, a new method based on EMD and Cohen's class distribution has been developed in this study. By simulating, this algorithm can eliminate the cross-terms in the time–frequency distribution satisfactorily, and can be applied in signal processing of track irregularities detection in high-speed train.

2. Signal acquisition

The axle box acceleration signals were acquired in a field test between two cities from Beijing to Tianjin in China. The GPS module was fixed on the top of the car-body in order to provide synchronization collection commands for all testing systems. The whole acquisition module included collecting, storing, transmitting, receiving and analysis modules. The power supply module was divided into two parts, one for acquisition and the other for GPS module. All the data were transmitted to the vehicle monitoring system via a wireless LAN. The EMUs needed to install equipment at no electricity area. And the tri-axial accelerations LC0715A were fixed on the axle box (Fig. 1), and which had to be calibrated and installed in advance. The vibration signals of the axle box were sent through the analog filter into the AD system amplified.

The intercity high speed railway employed the ballastless track and the steel rails of 100 m long, which was first time used in China. The length of the beams of bridges is 30 m long, and bridges are 84.2% of total length of the line. Fig. 2 shows the three groups of axle box acceleration signals in vertical orientation when the speed of the train was 100 km/h, 200 km/h and 300 km/h respectively. The sampling time was 2 s, and the sampling frequency was 4096 Hz. The data were tested for non-stationary.

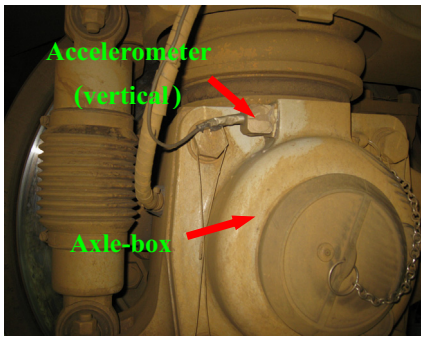

Fig. 1. Installation diagram of sensors fixed on axle box.

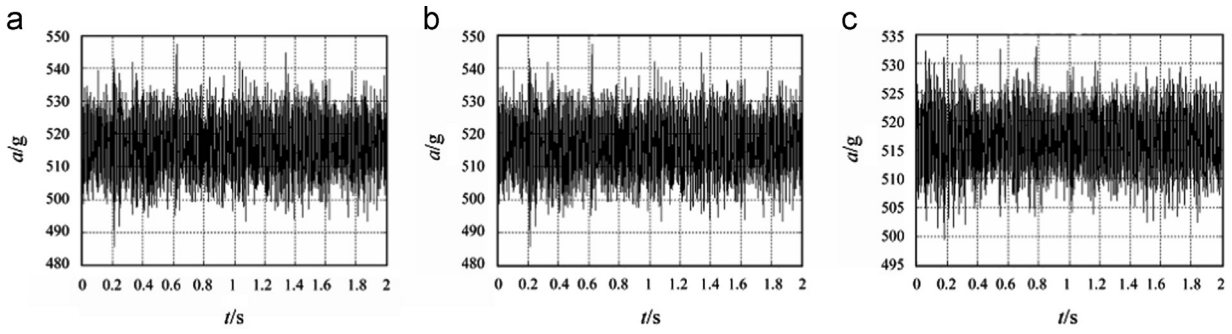

Fig. 2. Axle box acceleration signals.

3. Test signal analysis based on FFT and envelope demodulation

In the traditional way, test signals were analyzed by FFT and envelope demodulation method.

3.1. FFT

A fast Fourier transform (FFT) is an algorithm to compute the discrete Fourier transform (DFT). It has been described as "the most important numerical algorithms of our lifetime".

Let $x_0 \ldots x_{N-1}$ be complex numbers. The DFT is defined by the formula

$$X_k = \sum_{n=0}^{N-1} x_n e^{-j2\pi k \frac{n}{N}}, \quad k = 0 \ldots N-1 \tag{1}$$

where N is the sampling number.

Fig. 3a shows that when the train ran at the speed of 100 km/h, 75.5 Hz and 212 Hz were the obvious frequency ingredients. Fig. 3b shows that when the train ran at the speed of 200 km/h, the frequency of the acceleration signal was dispersed. There were nearly no main frequency ingredients. Fig. 3c indicates that when the speed came up to 300 km/h, the frequency of the acceleration signal was also dispersed. There were some frequency ingredients at 26.5 Hz, 87 Hz, and 200.5 Hz. In conclusion, when FFT is applied in total time domain or total frequency domain, we cannot get satisfactory results because the frequency characteristics of the axle box acceleration signals vary with time.

3.2. Envelope demodulation

For an amplitude-modulated signal $x(t)$, as

$$x(t) = A[1 + B\ \cos(2\pi f_n t)]\ \cos(2\pi f_z t) \tag{2}$$

where A is the amplitude of the signal, f_n is the modulation frequency, B is the modulation index, and f_z is the carrier frequency. Then

$$x(t) = A\ \cos(2\pi f_z t) + \tfrac{1}{2}AB\ \cos[2\pi(f_z - f_n)t] + \tfrac{1}{2}AB\ \cos[2\pi(f_z + f_n)t] \tag{3}$$

Considering the part of the positive frequency, we can have the FFT of $x(t)$, as

$$X_1(f) = \tfrac{1}{2}A\delta(f - f_z) + \tfrac{1}{4}AB\delta[f - (f_z - f_n)] + \tfrac{1}{4}AB\delta[f - (f_z + f_n)] \tag{4}$$

Based on this expression, the modulation signal includes the frequency components such as f_z, $f_z - f_n$, and $f_z + f_n$. The correspond amplitudes are $A/2$, $AB/4$, $AB/4$.

The Hilbert transform of function (2) is

$$\hat{x}(t) = A[1 + B\ \cos(2\pi f_n t)]\ \sin(2\pi f_z t) \tag{5}$$

The analytic function of $x(t)$ is

$$z(t) = x(t) + j\hat{x}(t) \tag{6}$$

So we can get the envelope of the signal $z(t)$, as

$$|z(t)| = \sqrt{x(t)^2 + \hat{x}(t)^2} = A|1 + B\ \cos(2\pi f_n t)| \tag{7}$$

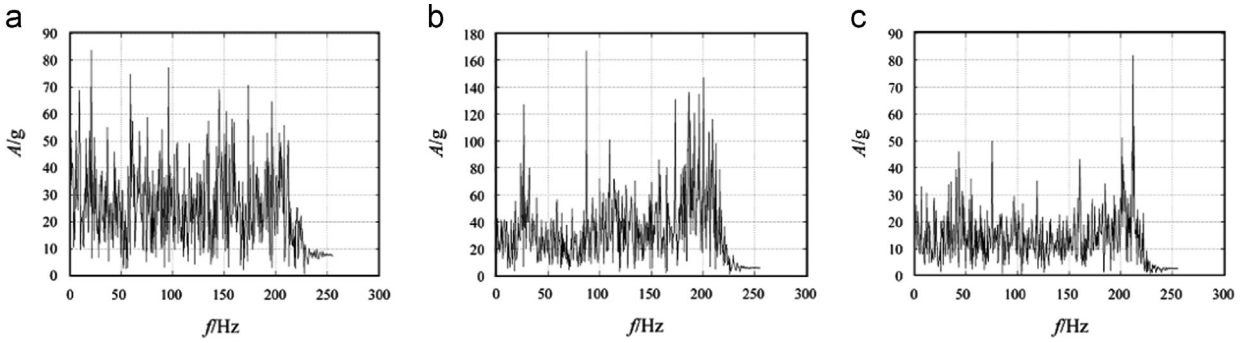

Fig. 3. FFT of the test signals.

For example, a cosine signal $f_1(t)=E\ \cos(\omega_0 t)$, we can get

$$f_2(t)=|f_1(t)|=\frac{2E}{\pi}+\frac{4E}{\pi}\ \cos(2\omega_0 t)-\frac{4E}{15\pi}\ \cos(4\omega_0 t)+\frac{4E}{35\pi}\ \cos(6\omega_0 t)-\ldots \tag{8}$$

Where there are only direct component and accidentally time component of ω_0. When

$$F_1(t)=E_0+E\ \cos(\omega_0 t),\quad 0<E_0<E \tag{9}$$

we can get

$$|F_1(t)|=|E_0+E\ \cos(\omega_0 t)|=c_0+c_1\ \cos(\omega_0 t)+c_2\ \cos(2\omega_0 t)+c_3\ \cos(3\omega_0 t)+\ldots \tag{10}$$

Based on the function (10), $|1+B\ \cos(2\pi f_n t)|$ from the function (7) can be expanded $z(t)$, as

$$z(t)=A|1+B\ \cos(2\pi f_n t)|=D_0+D_1\ \cos(2\pi f_n t)+D_2\ \cos(2\pi 2 f_n t)+D_3\ \cos(2\pi 3 f_n t)+\ldots \tag{11}$$

Then let the signal $z(t)$ passes a low-pass filter. We can get the modulation frequency f_n and its higher harmonic components $z(t)$, as

$$z(t)=D_0+\sum_{n=1}^{k} D_n\ \cos(2\pi n f_n t) \tag{12}$$

So the weak amplitude-modulated signals can be detected in the strong noise signals with the envelope demodulation method. As noise signals have a great influence on vibration signals, envelope demodulation is used for failure diagnosis on the train and rail.

The envelope spectrums of three groups of the acceleration signals are shown in Fig. 4. The frequency range of the band-pass filter is from 1200 to 1500 Hz. From Fig. 4a–c, there is no obvious spectrum and obvious modulation signals.

3.3. Summary

The axle box acceleration signals are non-stationary, and the non-stationary of the accelerations is emerged by track irregularities and the varying velocity. There is no valuable information by common FFT or envelope demodulation methods. So the time–frequency distribution method is used to analyze the axle box acceleration signals.

4. A new time–frequency analysis method

In time–frequency analysis method, Cohen's class has a high resolution. However, its application has been limited due to the presence of cross-term interference. EMD is an iterative process. The envelopes and their means are used to generate a collection of intrinsic mode functions (IMF). To minimize the cross-term interference, a new method based on EMD and Cohen's class distribution has been developed and it has been applied to analyze the track irregularities based on the axle box acceleration. Compared with the results by track inspection car, the consistent results appear, indicating that this approach can compensate some shortages of the track inspection vehicle, and it plays an important role in the high-speed and high-density test track irregularities.

4.1. Cohen's class

To reduce cross-term interference, many distributions such as the Choi–Williams distribution and the cone-shape distribution were developed. They can be expressed as a general formula:

$$P_x(t,f)=\frac{1}{2\pi}\iiint e^{-j2\pi\xi(t-u)}\varphi(\xi,\tau)x(u+\frac{\tau}{2})x^*\left(u-\frac{\tau}{2}\right)e^{-j2\pi f\tau}\,d\xi\,du\,d\tau \tag{13}$$

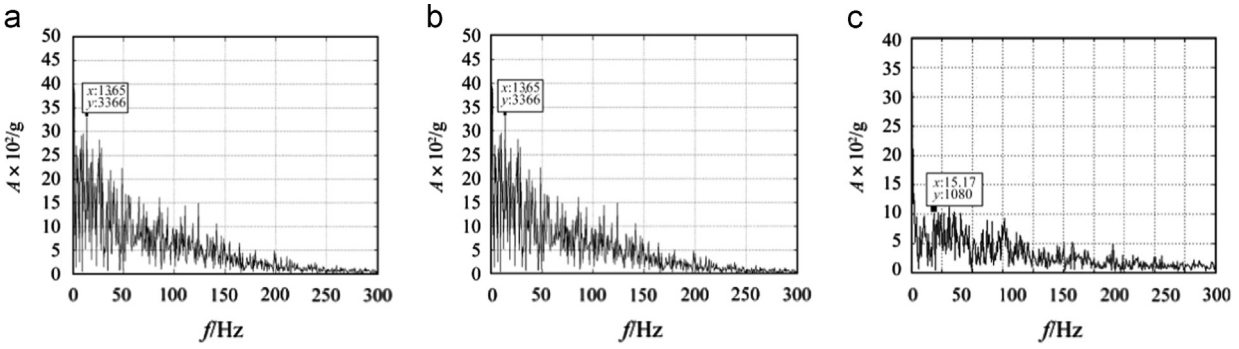

Fig. 4. Envelope spectrum of the test signals.

where $*$ is the plural conjugate, t is the time. $\varphi(\xi,\tau)$ is the kernel function, ξ is the frequency delay, and τ is the time delay. The performance of the bilinear time–frequency representation is determined by the kernel function. The requirements of the kernel function are both to minimize the cross-term and have a good feature.

4.2. Origin of the cross-term interference

A signal is practically the sums of single frequency signals. For a signal $x(t)$, as

$$x(t)=\sum_{k=1}^{n}x_k(t) \tag{14}$$

where $x_k(t)$ ($k=1, 2, \ldots, n$) is the single frequency signal. So the TFRs of the signal are as follows:

$$p_x(t,f)=\sum_{k=1}^{n}p_{x_k,x_k}(t,f)+\sum_{\substack{i=1\\ i\neq j}}^{n}\sum_{j=1}^{n}p_{x_i,x_j}(t,f) \tag{15}$$

$p_{x_k,x_k}(t,f)$ is the self-term of the bilinear time–frequency.
In formula (15)

$$p_{x_k,x_k}(t,f)=\frac{1}{2\pi}\iiint e^{-j2\pi\xi(t-u)}\varphi(\xi,\tau)x_k\left(u+\frac{\tau}{2}\right)x_k^*\left(u-\frac{\tau}{2}\right)e^{-j2\pi f\tau}\,d\xi\,du\,d\tau, \tag{16}$$

$$x_k(u+\tau/2)x_k^*(u-\tau/2)=\sum_{k=1}^{n}x_k(u+\tau/2)x_k^*(u-\tau/2) \tag{17}$$

$p_{x_i,x_j}(t,f)$ ($i\neq j$) is the cross-term of the bilinear time–frequency.
In formula (15)

$$p_{x_i,x_j}(t,f)=\frac{1}{2\pi}\iiint e^{-j2\pi\xi(t-u)}\varphi(\xi,\tau)x_i\left(u+\frac{\tau}{2}\right)x_j{}^*\left(u-\frac{\tau}{2}\right)e^{-j2\pi f\tau}\,d\xi\,du\,d\tau \tag{18}$$

$$x(u+\tau/2)x^*(u-\tau/2)=\sum_{k=1}^{n}x_k(u+\tau/2)x_k^*(u-\tau/2)+\sum_{\substack{i=1\\ i\neq j}}^{n}\sum_{j=1}^{n}x_i(u+\tau/2)x_j^*(u-\tau/2) \tag{19}$$

Cross-terms in the time–frequency distribution interfere with real energy distribution. Therefore, some efforts have been made to find methods to minimize the cross-term interference.

4.3. A new algorithm based on EMD and Cohen's class

EMD is a new method for analyzing non-linear and non-stationary data, which will generate a collection of intrinsic mode functions (IMF) [18]. The key part of the method is the "empirical mode decomposition", with which any complicated data set can be decomposed into a small number of intrinsic mode functions. This decomposition method is adaptive and highly efficient.

An IMF is a function that satisfies two conditions:

(1) In the whole data set, the number of the extreme points and the number of the zero points crossing the coordinate must either equal or differ at most by one.
(2) At any point, the mean value of the envelope defined by local maxima and minima is zero.

The most important step in the EMD method is the sifting process. Given a signal $x(t)$, the sifting process is defined by the following procedures:

1. Identify all the extreme points of the signal, interpolate between maxima points, and build the "envelope curves".
2. Interpolate between minima points, and build the "envelope curves".
3. Compute the mean m_1, and get $h_1=x(t)-m_1$. Ideally, h_1 should be the first IMF for $x(t)$.
4. If h_1 cannot satisfy all the requirements of IMF, the sifting process has to be repeated. In the second sifting process, h_1 is treated as the datum, and let $h_{11}=h_1-m_{11}$. This sifting procedure can be repeated k times, until h_{1k} is an IMF, that is $h_{1(k-1)}-m_{1k}=h_{1k}$. Then, it is designated as $c_1=h_{1k}$; the first IMF component from the data.

5. Subtract from the signal to obtain $r_1 = x(t) - c_1$ r_1. The second IMF can be obtained by repeating steps 1–4. By this way above, *n of the* IMFs are obtained. Then

$$\left.\begin{array}{l} r_1 - c_2 = r_2 \\ \vdots \\ r_{n-1} - c_n = r_n \end{array}\right\} \tag{20}$$

The sifting process can be stopped by any of the following predetermined criteria: (1) when the component c_n or the residue r_n becomes so small that it is less than the predetermined value of substantial consequence; (2) when the residue r_n becomes a monotonic function from which no more IMF can be extracted.

So for a multiple signal $x(t)$, the time-domain signal is separated into multiple IMFs using EMD:

$$x(t) = \sum_{i=1}^{n} c_i + r_n \tag{21}$$

In formula (21), c_i is the single signal component which satisfies the IMF condition and r_n is the residue of the mean trend of the signal.

To minimize the effect of the cross-terms, we propose an algorithm combining EMD with Cohen's class in this paper. The signal is decomposed into a sum of IMFs using EMD as a preprocessor at first. Then Cohen's class distributions of the IMFs are calculated. At last, sums of all Cohen's class distributions are acquired.

For a multiple signal $x(t)$, after EMD the TFRs are as follows:

$$P_x(t,f) = \sum_{k=1}^{n} p_{c_k,c_k}(t,f) \tag{22}$$

Compared with (15), the term $\Sigma_{i=1}^{n}\Sigma_{j=1}^{n} p_{x_i,x_j}(t,f)$ is eliminated. So the cross-terms are depressed.

4.4. Simulation

EMD is not an entirely mathematical model. It is empirical. So the time–frequency distributions of three typical simulation signals are calculated to indicate the accuracy of the proposed method. Compared with the Wigner–Ville distribution and Cohen's class distribution using generalized exponential kernel, the results show that this method can effectively suppress the cross-terms in the quadratic time–frequency distributions. The three typical simulation signals are used in it: a Gaussian linear frequency modulation signal, four Gaussian kernel signals and sine FM+hyperbola FM.

cross-terms are depressed. But the interference still exists. Figs. 5c, 6c and 7c are the TFRs combining EMD with Cohen's class. It almost contains auto-terms only. The cross-terms are eliminated. Compared with ideal results of time–frequency (Fig. 8), this method can minimize the cross-terms caused by the secondary distribution and a satisfactory result is acquired, which indicates that it is a good way for nonlinear and non-stationary signal analysis.

5. Test signal processing results

When the proposed method was applied to analyze the track irregularities based on the axle box acceleration (Fig. 9), it followed the steps below.

First, the axle box acceleration signals were preprocessed. In this process, the sampling frequency was decreased from 4096 Hz to 512 Hz by re-sampling and the trend term was removed. Secondly, the EMD method was used to realize self-adapting low-pass filtering. For example, Fig. 10 is the EMD reconstruction processing when the train ran at 200 km/h. 9 IMFs were obtained by EMD decomposition. Fig. 10b shows that the main frequency of the first 3 IMFs were beyond 50 Hz.

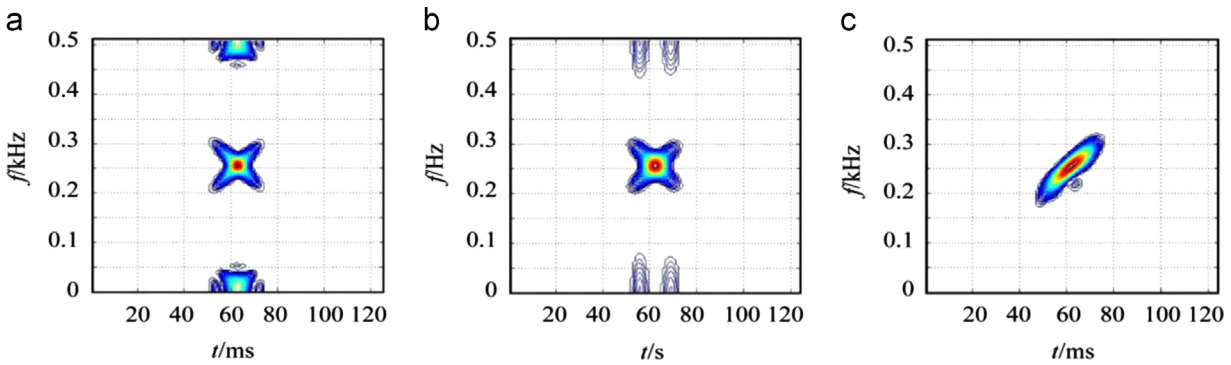

Fig. 5. Time–frequency distribution of a Gaussian linear frequency modulation signal for different methods.

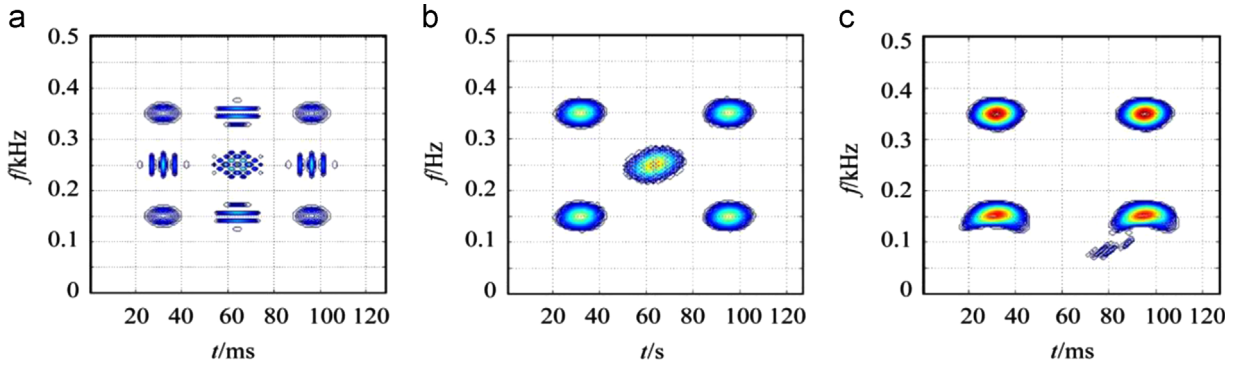

Fig. 6. Time–frequency distribution of the four Gaussian kernel signals for different methods.

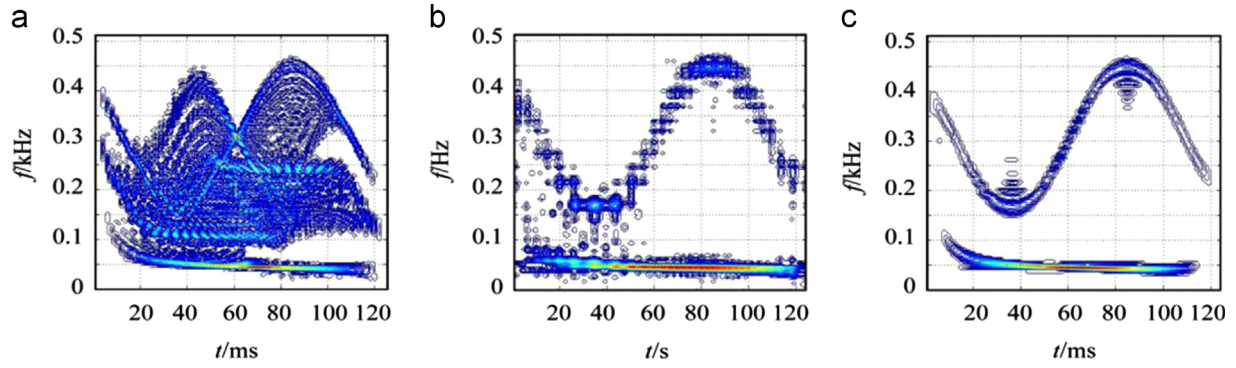

Fig. 7. Time–frequency distribution of the multiple signals for different methods.

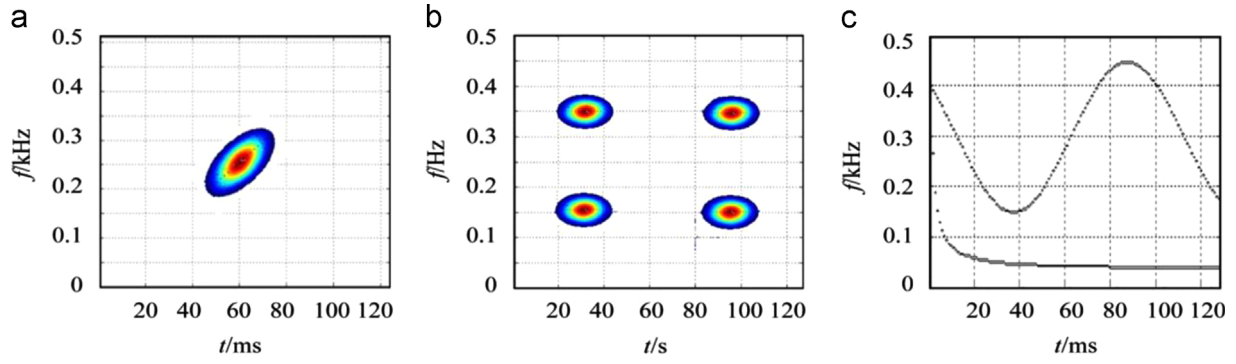

Fig. 8. Ideal time–frequency distribution of the simulation signals.

Fig. 9. Time–frequency analysis diagram of the test signals.

Considering the range of the axle box acceleration emerged by track irregularities below 50 Hz, the IMFs whose main frequency beyond 50 Hz were removed(in this case, the first 3 IMFs were removed). So Fig. 10b shows the EMD reconstructed result when the train ran at 200 km/h. At last, the filtered data were analyzed by the TFRs approach combined the EMD and Cohen's class which we developed above. Fig. 11b shows the TFRs of the axle box acceleration signals when the train ran at 200 km/h.

In the same way, the TFRs of the axle box acceleration signals when the train ran at 100 km/h (Fig. 11a) and 300 km/h (Fig. 11c) were gained.

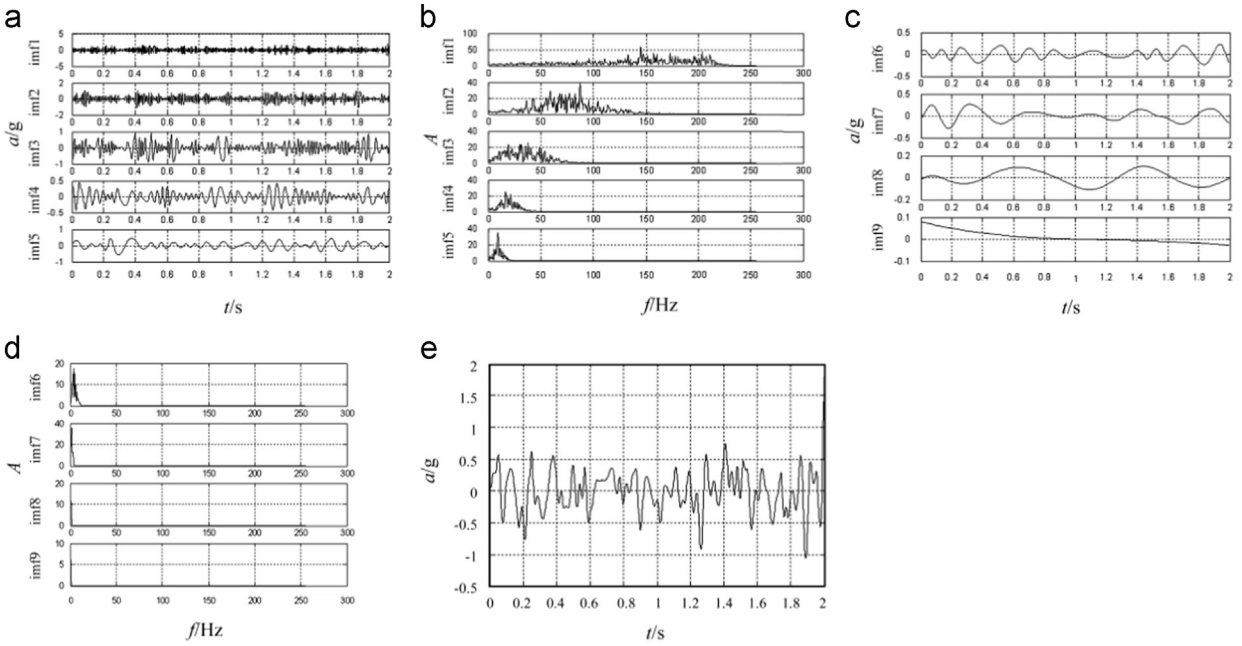

Fig. 10. EMD reconstruct ($v=200$ km/h).

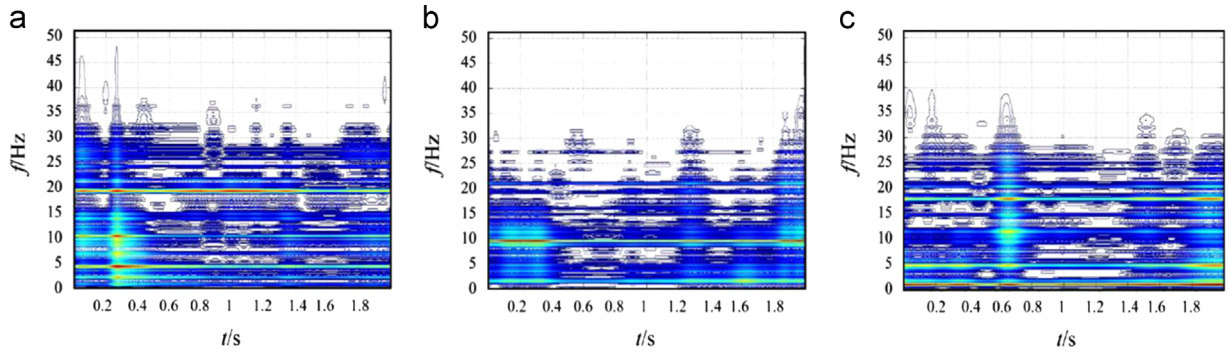

Fig. 11. TFRs of the axle box acceleration signals.

6. Discussion

6.1. Characteristic frequency

When $v=100$ km/h, the signals contain obvious periodic waves at $f_1=4.7$ Hz (Fig. 11a). When $v=200$ km/h, the signals contain obvious periodic waves at $f_2=1.5$ Hz and $f_3=9$ Hz (Fig. 11b). When $v=300$ km/h, the signals contain obvious periodic waves at $f_4=0.8$ Hz (Fig. 11c). From formula $\lambda=v/f$, the wavelength ingredients are $\lambda_1=6.68$ m, $\lambda_2=37$ m, $\lambda_3=6.17$ m, and $\lambda_4=104$ m. Table 1 shows the characteristic frequency of the axle box acceleration signals.

6.2. Wavelength analysis

From $\lambda=v/f$, the frequency is too little to observe in the frequency spectrum for long wave irregularity. So the time–frequency domain information in TFRS was used. From Fig. 11b, there are impulses in $t_1=0.2$ s and $t_2=1.9$ s. The time interval $\triangle t_1$ was 1.7 s or so. The velocity information $v=200$ km/h was collected by GPS. From the formula $\lambda=v\cdot t$, the space distance is $\lambda_4=94.4$ m. In the same way, from Fig. 11c, $\triangle t_2$ is 1.25 s or so, and $\lambda_6=104$ m. Table 2 shows the wavelength analysis of the axle box acceleration signals.

6.3. Resonance Frequency

In addition, when the speed was 100 km/h, 200 km/h and 300 km/h, the resonance frequencies of the axle box were 20 Hz, 10 Hz and 0.8 Hz respectively, which means that the resonance frequency reduced when the speed increased. Table 3 shows the resonance frequency of the axle box acceleration signals.

All the above conclusions (from Sections 6.1–6.3) about the track irregularities are obtained by axle box acceleration signals. Considering the variation of the train speed, and the time delay of the GPS, there are some errors about the results.

6.4. Comparisons

In [19], the track irregularities on the same line were analyzed by the track inspection cars, and some conclusions (Table 4) were acquired: (a) 6.5 m periodic waves in track profile irregularity are remarkable, which can cause the car body resonance in 10 Hz, when the train ran at 200 km/h, (b) 33 m periodic waves in the track profile irregularity are remarkable, (c) 100 m periodic waves in the track profile irregularity are remarkable.

From Table 1, $\lambda_1=6.68$ m and $\lambda_3=6.17$ m are very close to the $\lambda_{01}=6.5$ m (Table 4). This means there is 6.5 m periodic waves, which may be caused by the bogl slab up warp or supporting stiffness asymmetry. $\lambda_2=37$ m is very close to the $\lambda_{02}=33$ m (Table 4). This means that 33 m periodic waves in track irregularity are remarkable, which may be caused by the bridge up warp.

$\lambda_4=104$ m (Table 1), $\lambda_5=94.4$ m (Table 2) and $\lambda_6=104$ m (Table 2) are all close to $\lambda_{03}=100$ m (Table 4). There may be 100 m periodic waves. Because the ballastless track was welded with the steel rails 100 m long, it might be related to the quality of the seams of the ballastless track.

Table 1
Characteristic frequency of the axle box acceleration signals.

Velocity (km/h)	Characteristic frequency (Hz)	Wavelength (m)
100	$f_1=4.7$	$\lambda_1=6.68$
200	$f_2=1.5$, $f_3=9$	$\lambda_2=37$, $\lambda_3=6.17$
300	$f_4=0.8$	$\lambda_4=104$

Table 2
Wavelength analysis of the axle box acceleration signals.

Velocity (km/h)	Impulse signal time point (s)	Impulse signal space distance (m)
100		
200	$t_1=0.2$, $t_2=1.9$	$\lambda_5=94.4$
300	$t_3=0.65$, $t_4=1.9$	$\lambda_6=104$

Table 3
Resonance frequency of the axle box acceleration signals.

Velocity (km/h)	Resonance frequency (Hz)
100	$f_{r1}=20$
200	$f_{r2}=10$
300	$f_{r3}=0.8$

Table 4
Conclusions from the track inspection car.

Wavelength (m)	Resonance frequency(Hz)
$\lambda_{01}=6.5$	$f_{r1}=20$ ($v=200$ km/h)
$\lambda_{02}=33$	
$\lambda_{03}=100$	

In addition, when the speed is 200 km/h, the resonance frequency of axle box is at $f_{r2}=10$ Hz (Table 3) by the 6.5 m periodic waves, which is the same as $f_{r01}=10$ Hz (Table 4). That means that the uneven rail could cause a resonance between the bogie and vehicle body.

So compared with the results from track inspection car, the consistent results are obtained by the TFRS analysis. It indicates that this approach is correct and can compensate some shortages of track inspection vehicle.

7. Conclusions

Because of the cross-terms in time–frequency distribution, a method based on EMD and Cohen's class distribution is used. With this method the simulation signals of three different types are calculated. Compared with the result of WVD and Cohen's class distribution, this method can minimize the cross-terms caused by the secondary distribution and an ideal result of time–frequency analysis is acquired.

The proposed method has been applied to track irregularities signals analysis based on axle box acceleration. The results are in accordance with the track irregularities information getting from track inspection car. And when the time–frequency analysis method based on EMD and Cohen's class is applied, it makes up the deficiencies of online monitoring of the track irregularities of high density effectively. It has an important application value to track irregularities inspection of high speed and high density.

Acknowledgments

The authors are grateful for the financial support from the National Key Technology R&D Program of China (2009BAG12A01-E03, 2009BAG12A01-E02).

References

[1] H. Moritaka, T. Matsumoto, Track measurement by Kyushu Shinkansen cars in commercial service, in: B. Ning, C.A. Brebbia (Eds.), Computers in Railways Xii: Computer System Design and Operation in Railways and Other Transit Systems, Wit Press, Southampton, 2010, pp. 147–153.
[2] R. Insa, J. Inarejos, P. Salvador, L. Baeza, On the filtering effects of the chord offset method for monitoring track geometry, Proc. Inst. Mech. Eng. Part F-J. Rail Rapid Transit 226 (2012) 650–654.
[3] D.V. Popov, R.B. Ryabichenko, High speed imaging and processing for rail track inspection, Proc. SPIE (2005) 367–375.
[4] M. Bocciolone, A. Caprioli, A. Cigada, A. Collina, A measurement system for quick rail inspection and effective track maintenance strategy, Mech. Syst. Signal Proc. 21 (2007) 1242–1254.
[5] S. Bruni, F. Cheli, A. Collina, F. Resta, Road test data procedures for evaluating the Hunting instability threshold of a railway vehicle from on board measurements, Veh. Syst. Dyn. 33 (1999) 168–179.
[6] S.L. Grassie, Measurement of railhead longitudinal profiles. A comparison of different techniques, Wear 191 (1996) 245–251.
[7] M. Molodova, Z.L. Li, R. Dollevoet, Axle box acceleration: Measurement and simulation for detection of short track defects, Wear 271 (2011) 349–356.
[8] A. Lopez-Pita, P.F. Teixeira, C. Casas, L. Ubalde, F. Robuste, Evolution of track geometric quality in high-speed lines: ten years experience of the Madrid-Sevilleline, Proc. Inst. Mech. Eng. Part F-J. Rail Rapid Transit 221 (2007) 147–155.
[9] J.I. Real, L. Montalban, T. Real, V. Puig, Development of a system to obtain vertical track geometry measuring axle-box accelerations from in-service trains, J. Vibroeng. 14 (2012) 813–826.
[10] A. Caprioli, A. Cigada, D. Raveglia, Rail inspection in track maintenance: a benchmark between the wavelet approach and the more conventional Fourier analysis, Mech. Syst. Signal Process. 21 (2007) 631–652.
[11] M. Molodova, Z. Li, R. Dollevoet, D.W. Katholieke Univ Leuven, An investigation of the possibility to use axle box acceleration for condition monitoring of welds, Proc. ISMA (2008) 2879–2886.
[12] Z. Li, M. Molodova, R. Dollevoet, High frequency axle box acceleration for early detection of squats: numerical simulation, Proc. IWSHM (2011) 815–822.
[13] P. Gullers, L. Andersson, R. Lunden, High-frequency vertical wheel-rail contact forces – field measurements and influence of track irregularities, Wear 265 (2008) 1472–1478.
[14] J.S. Lee, S. Choi, S.S. Kim, C. Park, Y.G. Kim, A mixed filtering approach for track condition monitoring using accelerometers on the axle box and bogie, IEEE Trans. Instrum. Meas. 61 (2012) 749–758.
[15] Z.L. Cao, The analysis of the simulation test and characteristics of the vibration states of rolling stock, Rolling Stock (1994) 1–4.
[16] X.B. Liu, Method for picking up rail wavy irregularities based on empirical mode decomposition method, China Railway Sci. (2006) 26–30.
[17] X.S. Jin, L. Wu, J.Y. Fang, S.Q. Zhong, L. Ling, An investigation into the mechanism of the polygonal wear of metro train wheels and its effect on the dynamic behaviour of a wheel/rail system, Veh. Syst. Dyn. 50 (2008) 1817–1834.
[18] E.H. Norden, S. Zheng, R.L. Steven, The empirical decomposition and the Hilbert spectrum for non-linear and non-stationary time series analysis, Proc. R. Soc. (1998) 903–995.
[19] S.G. Zhang, X. Kang, X.B. Liu, Characteristic analysis of the power spectral density (PSD) of track irregularity on Beijing–Tianjin inter-city railway, China Railway Sci. 101 (2008) 25–30.